PEER-REVIEWED Version https://doi.org/10.1016/j.fusengdes.2021.112999

Mechanical impact of electromagnetic transients on the European DEMO divertor. Part 1: Vertical Displacement Event

G. Di Mambro[a,b], A. Maffucci[a,b], G. Mazzone[c], S. Ventre[a,b], F. Villone[a,d], J.H. You[e]

[a] CREATE Consortium, Via Claudio 21, 80125 Naples (Italy)

[b] DIEI, Dept. of Electrical and Information Engineering, University of Cassino and Southern Lazio, Via G. Di Biasio 43, 03043, Cassino (FR), Italy

[c] ENEA, Dept. of Fusion and Technology for Nuclear Safety and Security, Via Fermi 45, 00044 Frascati (RM), Italy

[d] DIETI - Dept. of Electrical Engineering and Information Technology, University of Naples Federico II, Via Claudio 21, 80125 Naples (Italy)

[e] Max Planck Institute for Plasma Physics, Boltzmann str. 2, 85748 Garching, Germany

Corresponding author: Gennaro Di Mambro, mail to: gennaro.dimambro@unicas.it

ABSTRACT

This paper presents the study of the forces and moments expected on the European DEMO divertor, due to the fast electromagnetic transients associated to plasma instabilities events. A 3D Magneto-Quasi-Static (MQS) model is here adopted to solve such a problem, implemented in Ansys EMAG. A hybrid modelling approach is proposed, that can be placed between a pure global model (where the divertor is modelled along with all the external passive and active components) and a local one, where only the divertor is present in the model and the external world is represented through equivalent boundary conditions (submodelling). Indeed, the model proposed here includes a detailed description of all the divertor components (cassettes, targets, liner, cooling pipes, etc..) and a coarser description of the main passive external components (vessel, blanket, rails, etc..). The active components (coils and plasma currents) are instead replaced by suitable equivalent current sources and by a known equilibrium magnetic field. The analysis is here carried out with reference to one of the most challenging events for the divertor, namely a downward directed Vertical Displacement Event. The forces and moments associated to the whole divertor and to its cooling subsystem are evaluated, and a sensitivity analysis is performed to check the impact of the choice of the materials to be used to realize the supports inside the divertor and between the divertor and the vacuum vessel.

KEYWORDS

European DEMO, Divertor, Electromagnetic forces, eddy-currents, halo-currents, plasma disruptions

1. INTRODUCTION

The mechanical consequences of plasma instabilities events have to be accurately taken into account in the design of a tokamak. Indeed the interaction between the magnetic field and the huge electrical currents flowing into the conducting structures as a consequence of such instabilities (such as eddy currents and halo currents) gives rise to strong electromagnetic (EM) loads, possibly accompanied by mechanical deformations and widespread damages.

In this paper, we analyse the EM loads expected on the divertor of the European DEMOnstrator Fusion Power Plant [1]-[3] (hereafter, EU-DEMO), undergoing to plasma instabilities events. This work has been carried out in the frame of the Pre-Conceptual Design phase of EU-DEMO divertor [4]. The analysis is performed by means of a Finite Element (FE) 3D Magneto-Quasi-Static (MQS) model.

Previous works with transient EM analysis of the EU-DEMO divertor have been so far carried out, with reference to the baseline divertor design available at that time, as for instance [5]-[7]. In [5], a holistic pre-conceptual design is discussed and the main technological solutions are investigated in terms of neutronic, thermal, hydraulic and electromagnetic behaviour. In [6]-[7], a simplified version of the divertor is included into a global model, containing a sector of the machine with all the relevant external components, both passive (blanket, vessel, etc.) and active (coils). As done also in the present paper, the EM analysis in [6]-[7] is carried out in a 22.5° toroidal sector of the machine, by exploiting symmetric boundary conditions on the cutting surfaces (the two poloidal external planes). In such a sector, three divertor modules are hosted, that are modelled together with the Vacuum Vessel (VV), the inboard, outboard and central blankets modules, and the equatorial and upper port extensions. As for the excitations, the Poloidal Field Coils (PFCs) and the Toroidal Field Coils (TFCs) are included in the model, along with the Poloidal Field Variation Coils (PFV) and the Toroidal Field Variation Coils (TFV) as excitations. The model is used to estimate the EM loads due to Vertical Displacement Events (VDEs) and TF Coil Fast Discharge loads (TFCFD). In addition, different configurations of the electrical contacts between blankets and vessel and between upper plugs and port walls are analysed.

The work in [8] is also performed with a global model including a simplified version of the divertor. The work is aimed not only at evaluating the capacity of the structures included in the model to withstand the EM loads, but also at reducing the model uncertainties related to the input data coming from the plasma instability analysis.

Alternative approaches have been proposed, based on analytical estimations, such as that proposed in [9] to evaluate the impact of the EU-DEMO Tokamak aspect ratio on the EM loads. Specifically, three values for the aspect ratio are considered, A=2.6, 3.1 and 3.6, and the EM loads are obtained with reference to VDEs, and TFCFDs. In [9] it is shown that for VDEs, the higher loads are associated to the downward net vertical forces and the aspect ratio has a lower impact on these loads, compared to those of other events.

A more detailed version of EU-DEMO divertor is introduced in [10], where the cassettes and the water cooling pipes are present. The work is focused on the analysis of the paths of the currents along the divertor subsystems, with the determination of an equivalent electrical resistance (shunt resistance). The model adopted here is a full local model, where only the divertor components are included, and the excitations coming from the analysed plasma event are represented through two known currents directly imposed to the same area of the water cooling pipes (a VDE current, modelling the eddy currents, and a thermo-current, representing the halo currents).

A different approach is followed in the work [11], which however refers to the K-DEMO reactor. The divertor EM response to a major disruption (MD) is indeed derived by using a global model including the same passive and active elements as previously described for [6], [7], with the addition of the plasma itself. The plasma data associated to the chosen event are used to define a body force load to be associated to each element used in the FEM analysis.

In this paper, a study of the EM forces on the EU-DEMO divertor is carried out with reference to VDE instabilities, and specifically to a downward VDE. Indeed, such an event is of particular interest for the divertor integrity being a fast event, with the plasma current hitting directly the upper parts of the divertor assembly.

A hybrid modelling approach is adopted, where the divertor is modelled in detail (by using the present release of the CAD design [12]), and the main external passive components are included, such as vessel and blankets.

The model and the sources are described in Section II. In Section III the results of the EM transient analysis are presented and discussed, by studying the obtained distributions of eddy currents and force densities. The resultant of forces and torques on the whole divertor assembly and on its subparts are also reported, along with a sensitivity analysis of the impact of the conductivity values of some supporting parts.

2. EM Model of the Divertor

As pointed out in the Introduction, in this paper a hybrid modelling approach is adopted, since the proposed model settles between a local and a global one. In a local

 https://doi.org/10.1016/j.fusengdes.2021.112999

model, only the divertor would be included and the effect of the external world would be represented through suitable boundary conditions at the cutting boundary, as in the zooming or submodelling approaches. In a global model, all the passive and active components would be considered, such as for instance vessel, blankets, PFCs and TFCs. The model adopted in this paper includes the divertors (with finer details on its subparts) and the main external passive components such as VV, blanket modules, rails (with a coarser description), see Fig.1. The model does not contain active components such as PFCs and TFCs, and the excitation is provided by suitable sets of equivalent currents imposed on two layers (PFV and TFV) and by a known equilibrium magnetic field.

2.1 Geometry and materials

A toroidal sector of 22.5° is assumed (Fig.1), that is a suitable choice for performing a 3D EM analysis of the whole machine, assuming rotational symmetry and imposing periodicity conditions.

The CAD model includes three divertor modules, the blanket, the Vacuum Vessel (VV), and the inward and outward divertor supports to VV. The details of a single divertor module are visible in Fig.2. The electrical properties of the materials used for the model components are listed in Table 1, taken from [13]-[16].

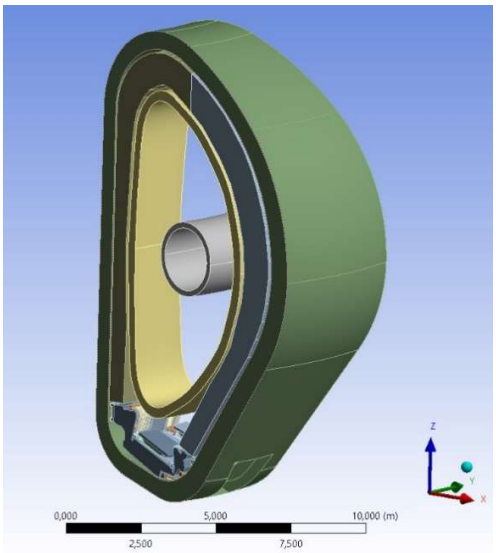

Fig. 1. The analyzed 22.5° sector of DEMO in-vessel assembly, including the divertors, blankets, vessel and the two layers where the equivalent current sources are imposed.

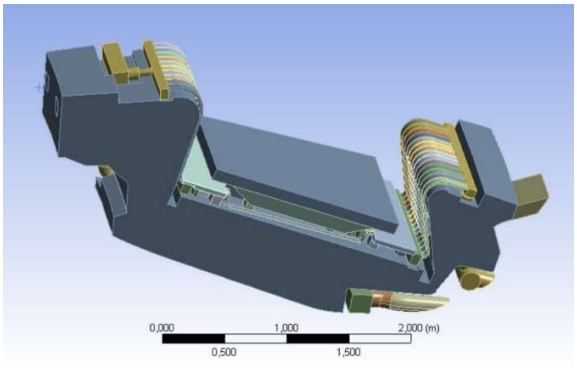

Fig. 2. CAD model of a single divertor module.

Table 1. Model components and materials properties [13]-[16]

Component	Material	Resistivity (Ωm)	Relative Permeability
Vessel	AISI 316 L(N) IG	$7.59 \cdot 10^{-7}$	1
Blanket	EUROFER97	$8.54 \cdot 10^{-7}$	39 – 53
Divertor cassette	EUROFER97	$8.54 \cdot 10^{-7}$	39 – 53
Cassette support to VV (inward)	AISI 316 L(N) IG	$7.59 \cdot 10^{-7}$	1
Cassette support to VV (Wishbone)	Ti-6Al-4V	$1.5 \cdot 10^{-6}$	1
Pipes, manifolds, and supports of cooling system	AISI 316 SS	$7.59 \cdot 10^{-7}$	1
Cooling pipes (vertical targets)	CuCrZr	$2.33 \cdot 10^{-8}$	1

The following simplifying assumptions have been made:

- the VV is a simplified version of the actual one, including the downward hole corresponding to the lower port, retaining the double-shell steel structure with a thickness of 6 cm;
- the blankets have been modelled as bulk structures: equivalent conductivity and permeability values have been used to consider the void ratio. They are made of two different pieces, respectively in the inboard and outboard sides. The supports that electrically connect the blankets to the vessel are also included;

 https://doi.org/10.1016/j.fusengdes.2021.112999

- the divertor cassettes have been modelled as bulk conducting materials: equivalent conductivity and permeability values have been used to take into account the original ratio between vacuum and steel volumes. The cassette-to-VV inward and outward supports have been properly included;
- the cooling pipes of the vertical targets have been simplified. Each three pipes in the original CAD has been grouped into an equivalent pipe, with the same cross section of the original three pipes, hence the final volume is left unchanged. All the small pipes (e.g., the pipes that bring water to shielding liners) have been modeled as a bulk conductor. An equivalent conductivity value has been used to take into account the original ratio between water and steel volumes.

As shown in Table 1, the blanket and cassette modules (made by EUROFER97) exhibit magnetic properties [16].

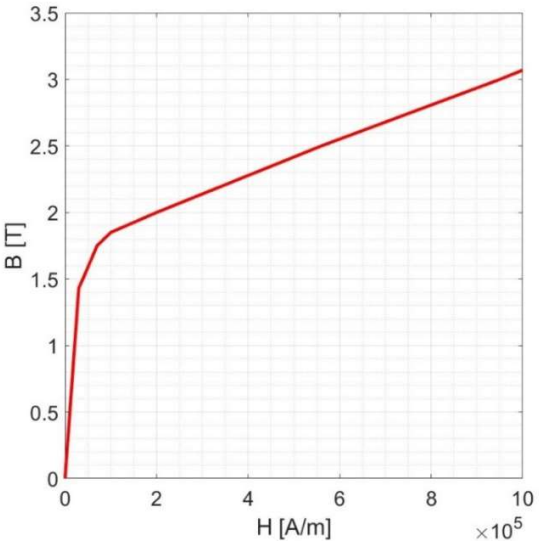

Fig. 3. B-H magnetization curve of the Eurofer97 steel [16].

Table 2. Expected ranges of the static magnetic flux density in the magnetic components of the model, for the studied event.

Component	B_{min} [T]	B_{max} [T]
Divertor Cassettes	4.81	8.20
Outer Blanket Module	3.38	5.06
Inner Blanket Module	4.97	8.57

The B-H magnetization curve of such a material (reported in Fig.3) is derived from the data provided in [17]. For such a material, the relative permeability associated to the linear tract of this curve is reported to fall in the range 39-53, also depending on the actual temperature [16]. The saturation can be assumed to occur for a level of magnetic flux density $\boldsymbol{B}$ approximately equal to 3T. Note that both the permeability in the linear tract and the saturation field can change as an effect of neutron irradiation. Although no specific work is available on the EUROFER97, the results provided in [18] with reference to magnetic steels adopted for nuclear vessels suggest that a neutron irradiation may change the B-H response. Specifically, after irradiation, the permeability in the linear tract is lower and the saturation occurs for lower values of the magnetic field.

However, all the above considerations do not have a significant impact in our work, since for the transient event considered in this paper (VDE, see subsection 2.2), the expected values of the static magnetic flux density in the magnetic regions (see Table 2) bring these components to work in a magnetic saturation condition.

2.2 Excitation sources and plasma events

In this paper, we analyze a downward Vertical Displacement Event (VDE_DOWN_74ms, whose details can be found in [3]), that is a plasma instability of particular interest for the divertor integrity, as pointed out in the introduction. Specifically, the chain of events is as it follows. A plasma event characterized by a sudden variation of poloidal beta (a glitch) triggers the VDE, so that the plasma moves vertically (exponentially) downwards, until it hits the first wall. When boundary safety factor drops below 2, the Thermal Quench (TQ) occurs, lasting 4 ms. During this fast phenomenon, a current density flattening occurs [19]. As a consequence, the plasma internal inductance decreased abruptly, leading to a spike of plasma current around 5% to approximately guarantee magnetic flux conservation inside the plasma. Immediately after, a linear Current Quench (CQ) takes place, bringing the toroidal current to zero in 74 ms. This QC event has been chosen since it is among the fastest ones predicted for EU-DEMO, by extrapolation and scaling of experimental results obtained in other machines [19].

 https://doi.org/10.1016/j.fusengdes.2021.112999

Note that the plasma undergoes progressive changes of topology: starting from a single null configuration, it hits the wall outboard and gets limiter; then, due to TQ+CQ, the plasma "shrinks" and gets diverted again, so that it moves downwards with an X-point configuration. Eventually it touches the wall in the divertor region, switching again to a limiter configuration (Fig. 4).

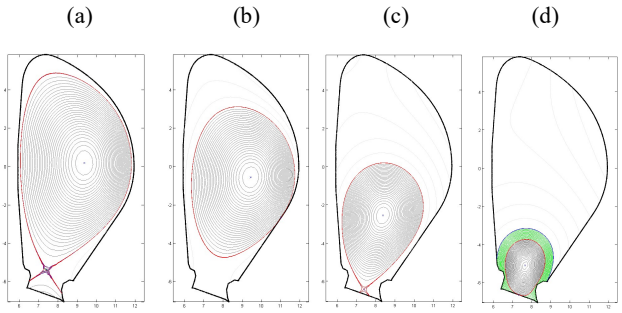

Fig. 4. Snapshots of the plasma configurations for the event VDE_DOWN_74ms, at the time instants: (a) t=0s; (b) t=1.53s; (c) t = 1.65s; (d) t = 1.67s.

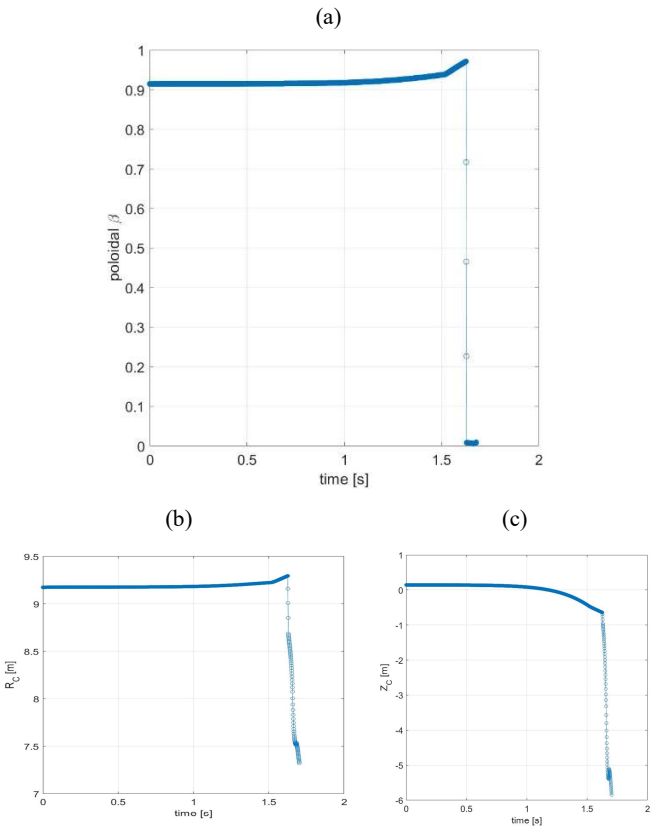

Fig. 5. Time evolution of (a) the poloidal beta, and (b), (c) the radial and vertical coordinates of the plasma centroid, during the VDE_DOWN_74ms event.

At that time, the q_95 safety factor (i.e. the safety factor of the magnetic surface enclosing 95% of the total poloidal flux) is around 2.4. The time evolution of poloidal beta and of the radial and vertical coordinates of the plasma centroid are reported in Fig.5.

The plasma simulations have been carried out with the CarMa0NL code [20]. This computational tool describes the electromagnetic interaction of the plasma with the surrounding structures via a set of suitable filamentary currents, located on a fixed surface, whose time-varying values are found imposing that they provide the same poloidal magnetic field as the plasma on the structures. In this sense, we can state that these currents are equivalent to the plasma and are used in the present paper as the PFV (Poloidal Field Variation) set of current, flowing in the outer layer depicted in Fig. 6. Another source of eddy currents is the time variation of the plasma toroidal flux. By using this quantity, as provided by CarMa0NL, it is possible to derive the TFV (Toroidal Field Variation) set of currents, to be associated to the inner layer in Fig. 6. The time-domain evolution of the total equivalent current flowing into the PFV coils and of the plasma toroidal flux are given in Fig.7, for the considered event.

In addition, the model excitations are completed by the inclusion of the Halo currents, directly injected in the components located in the lower part of the studied assembly, hit by the plasma during the evolution of the instability event. Also, this quantity is computed by CarMa0NL (green region in Fig, 4d) and used as input.

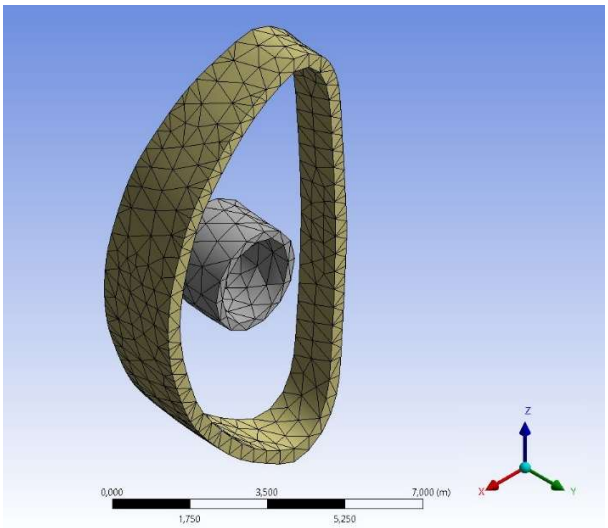

Fig. 6. Eddy-current problem excitation. Outer layer: PFV equivalent currents; inner layer: TFV equivalent currents.

https://doi.org/10.1016/j.fusengdes.2021.112999

The spatial distribution of the currents injected into the main components of the model is given in Fig.8, that includes the divertor liner and the bottom parts of the outward and inward blanket modules. For the same event, the total Halo current injected into three divertor modules hosted in the analyzed sector is shown in Fig.9. The PFV and TFV excitations start approximately at t=1.63s, while the Halo currents start later, as expected, at t = 1.66 s.

Note that the above three equivalent sources take into account in their spatial and temporal variation the spatio-temporal evolution of the plasma current, including the motion of the plasma inside the vessel.

Finally, CarMa0NL also provides the static equilibrium field due to PF and TF coils. Being time constant, this field does not induce eddy currents, but it must be accounted for in the computation of the electromagnetic force, as it will be detailed in Section 3.

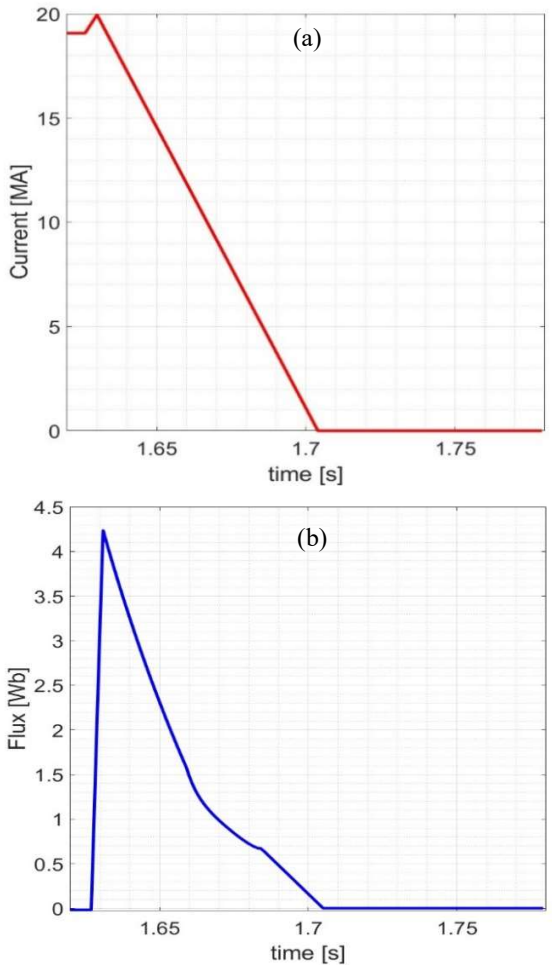

Fig. 7. Time evolution of: (a) the total equivalent PFV current; (b) the variation of the plasma toroidal flux (VDE_DOWN_74ms).

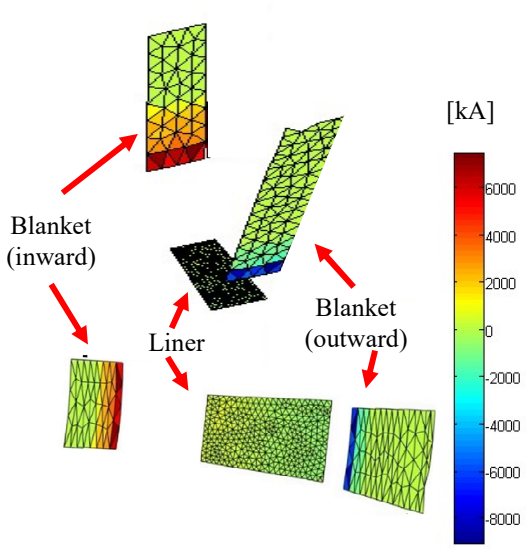

Fig. 8. Spatial distribution of the Halo currents injected into some of the main components of the model: inward and outward blanket module, divertor liner. Event: VDE_DOWN_74ms, time: 1.68 s.

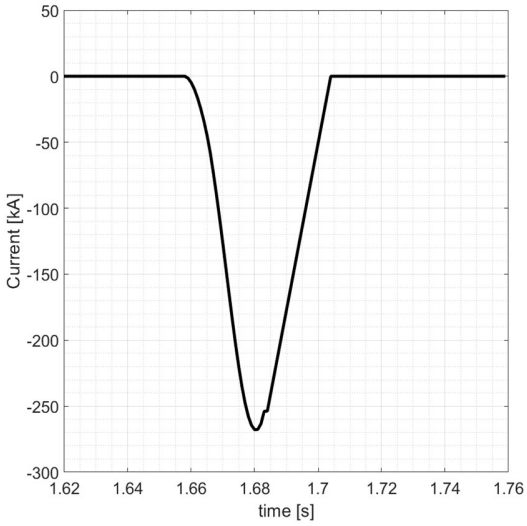

Fig. 9. Time domain evolution of the total halo current injected into the blankets and the three divertors (VDE_DOWN_74ms).

2.3 Numerical model and load evaluation

As pointed out in the Introduction, the electromagnetic problem was here formulated by means of the Magneto-Quasi-Static (MQS) model. In this model, the electromagnetic induction (e.g., the effect of the time variation of the flux of **B** field is rigorously taken into account, whereas it is neglected the effect the time variation of the flux of **D** field). As a consequence, eddy currents induced in the conducting structures are rigorously modelled, whereas displacement currents are neglected.

 https://doi.org/10.1016/j.fusengdes.2021.112999

The EM analysis is here performed in ANSYS EMAG (Release 2019.R2), [21]. An adaptive and conformal meshing is used, based on tetrahedrons: a meshed divertor is depicted in Fig. 10. Specifically, the 8-nodes element type SOLID97 is used, suitable for the eddy-current transient analysis based on the magnetic vector potential formulation with the Coulomb gauge. Here, 4 degrees of freedom per node are used: the magnetic vector potential (A_X, A_Y, A_Z), and the electric scalar one (VOLT).

The adopted mesh statistics are reported in Table 3a: the mesh has 402705 nodes and 290876 elements. The quality of the mesh is checked by evaluating a metric that is calculated from the shape of each single element [21]: the closer to 1 is this index, the better is the quality. The distribution of the element metrics among the mesh is reported in Fig. 11 and shows a good quality (the average value for such an index is about 0.66, with a standard deviation of 0.21). To ensure the reliability of the numerical results, a mesh assessment is performed, by building a finer mesh, whose statistics are reported in Table 3b. Despite the number of nodes and elements is more than doubled passing from the reference mesh to the finer one, the maximum error in evaluating of the peaks of the forces (see Section 3) was found to be less than 4%.

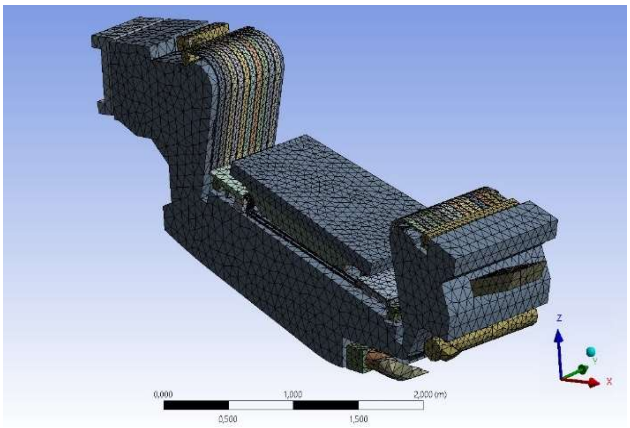

Fig. 10. View of the meshed divertor assembly.

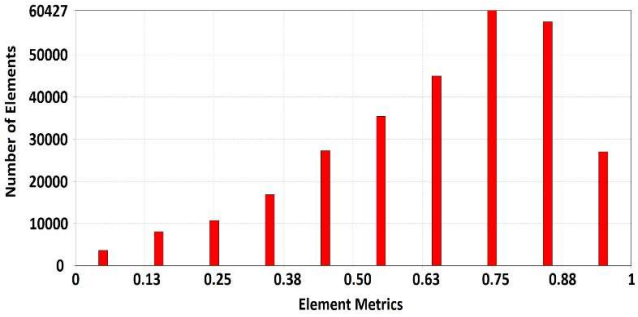

Fig. 11. Evaluation of the element metrics for the adopted mesh.

Table 3a. Statistics for the adopted mesh.

Statistics	
Nodes	402705
Elements	290876
Mesh Metric	Element Quality
Min	5,62354126322783E-04
Max	0,999908251397524
Average	0,654762325435997
Standard Deviation	0,21105564353585

Table 3b. Statistics for the finer mesh (mesh assessment)

Statistics	
Nodes	864989
Elements	635692
Mesh Metric	Element Quality
Min	5,34838405753726E-04
Max	0,999911019487932
Average	0,725472040655438
Standard Deviation	0,192755524930765

3. Results and Discussion

3.1 Lorentz force model

The transient analysis carried out with the model described here provides the time-domain waveforms of the density of currents (both eddy and Halo currents) in the conducting regions of the divertor, $\boldsymbol{J}(x,y,z,t)$ and of the magnetic induction field associated to the imposed excitations, $\boldsymbol{B}(x,y,z,t)$. Note that to this field it muste be added the static contribution associated to the equilibrium field due to PF and TF coils, as pointed out in Section 2, say $\boldsymbol{B_0}(x,y,z,t)$. Therefore, the forces and moments are to be computed by using the total field, defined as:

$$\boldsymbol{B_{tot}}(x,y,z,t) = \boldsymbol{B}(x,y,z,t) + \boldsymbol{B_0}(x,y,z,t). \qquad (1)$$

The volumetric density of Lorentz forces are then calculated as it follows:

$$\boldsymbol{f_{tot}}(x,y,z,t) = \boldsymbol{J}(x,y,z,t) \times \boldsymbol{B_{tot}}(x,y,z,t), \qquad (2)$$

being × the symbol of the vector product. The resultant forces are calculated by integrating the force density (2) in the volume of interest (the whole divertor and/or any of its subcomponents). In addition, the resultant moments of forces are calculated with reference to the Geometric Mass Center (GMC) of the component of interest.

3.2 Distribution of the current densities

The results of the transient analysis for the considered event (VDE_DOWN_74ms) are reported in Figs.12 and 13,

 https://doi.org/10.1016/j.fusengdes.2021.112999

where the distributions of the current densities are shown on the divertor cassettes (Fig.12) and on the cooling subsystem (Fig.13). These distributions refer to the time instants at which the peaks of forces occur, see subsection 3.3. It can be noticed that the current density is closing local loops in the internal and external parts of both the body cassettes (Fig. 12) and on the cooling system (Fig. 13). The main reason for these loops is the effect of the different values of the electrical resistivity associated to the components. Indeed, the tubes of the vertical targets (PFC) are made by CuCrZr, that has a lower resistivity compared to the materials used for the supports and the cassettes (AISI), as shown in Table 1.

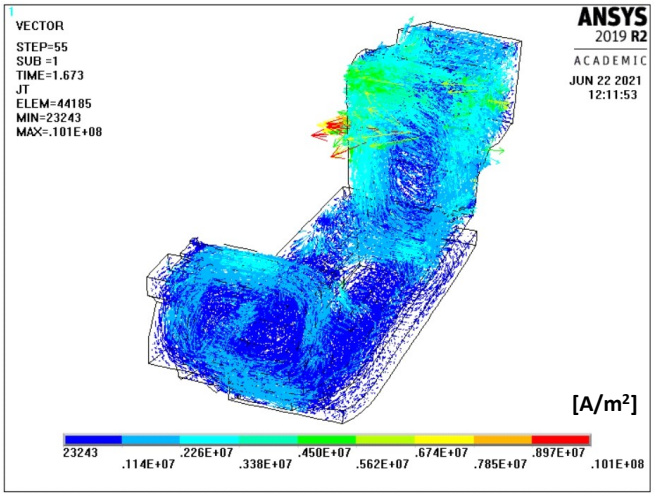

Fig. 12. Current density distribution on the cassette body, at the time instant of the maximum Lorentz force (1.673 s).

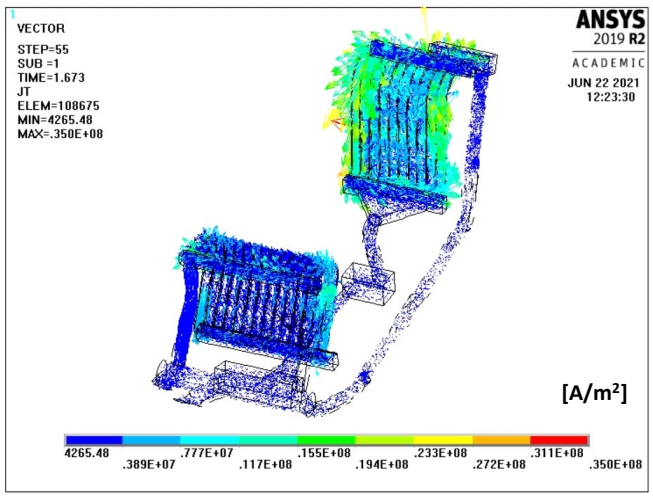

Fig. 13. Current density distribution on the cooling pipe, at the time instant of the maximum Lorentz force (1.673 s).

3.3 Evaluation of forces and moments

Starting from the results of the previous subsection, the resultant Lorentz forces and moments are derived for the considered event. The results related to the whole divertor assembly are shown in Figs.14 and 15, whereas those associated to the cooling subsystem are reported in Figs.16 and 17. The latter is composed by all the cooling pipes in CuCrZr and all manifolds in AISI 316. The results refer to one of the lateral divertors.

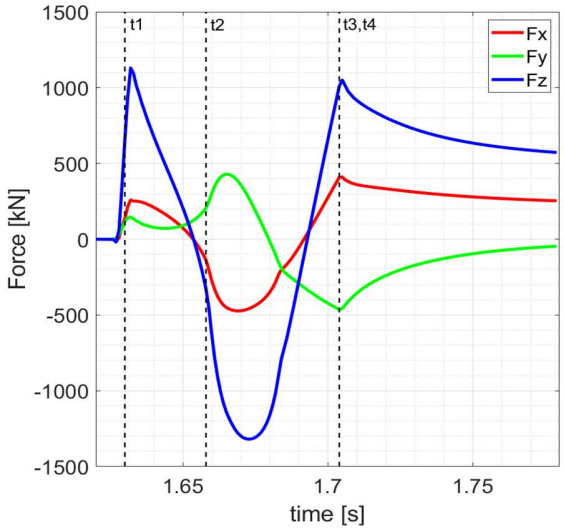

Fig.14. Time-domain evolution of the resultant of Lorentz's forces on the whole divertor (VDE_DOWN_74ms event). The following time instants are highlighted: t_1 = start of Current Quench; t_2 = start of Halo currents; t_3 = t_4 end of CQ and Halo.

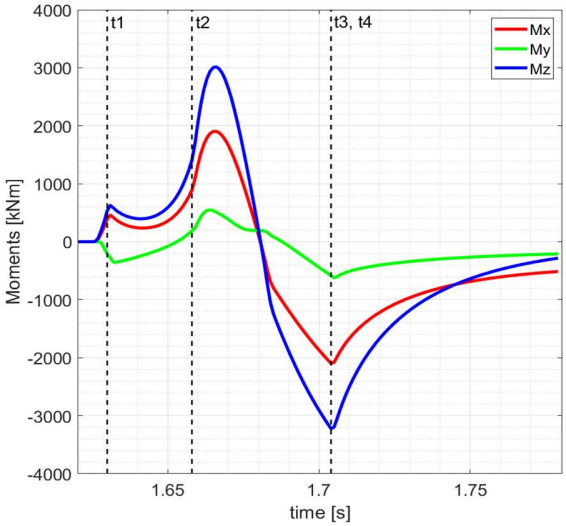

Fig.15. Time-domain evolution of the resultant of the moments on the whole divertor (VDE_DOWN_74ms event). Time instants t_1, .., t_4 as in Fig.14.

 https://doi.org/10.1016/j.fusengdes.2021.112999

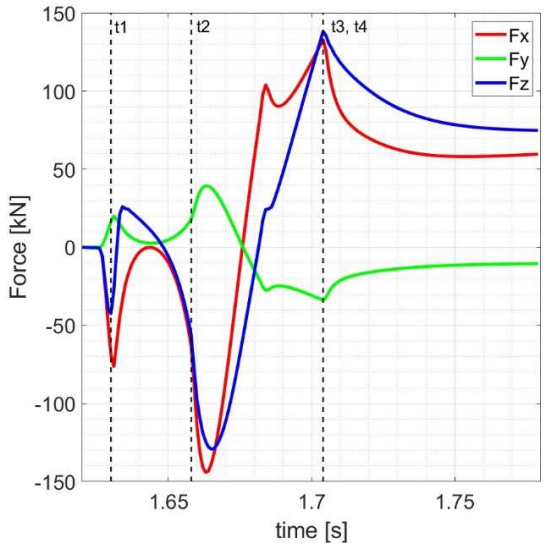

Fig.16. Time-domain evolution of the resultant of Lorentz's forces on the cooling system (VDE_DOWN_74ms event). Time instants t_1, .., t_4 as in Fig.14.

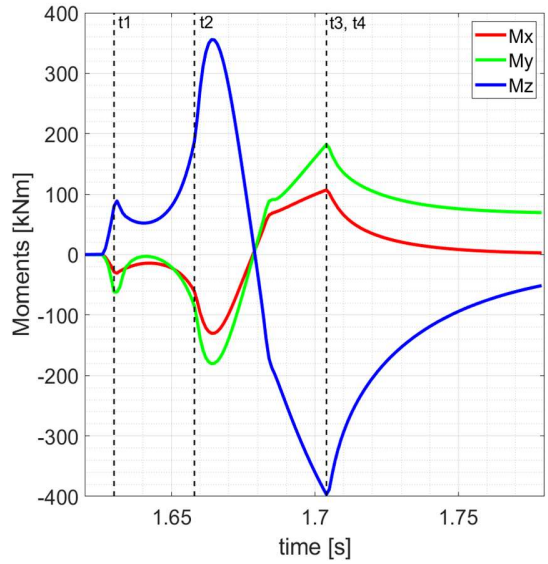

Fig.17. Time-domain evolution of the resultant of the moments on the cooling system (VDE_DOWN_74ms event). Time instants t_1, .., t_4 as in Fig.14.

Table 4. Peak values of the resultants of Lorentz's forces and moments for the VDE_DOWN_74ms event.

	Fx [kN]	**Fy [kN]**	**Fz [kN]**	**Mx [kNm]**	**My [kNm]**	**Mz [kNm]**
Divertor	-442.5	-451.3	-1283	-2104	-542.81	-3183
Cooling	-127.4	34.17	125.3	-113.0	-154.71	-314.5

The x-, y- and z- components of forces and moments correspond to the radial, toroidal and vertical components, respectively (the global reference system is adopted). The moments are computed with respect to the center of mass of each system: x=7.2513m, y=-0.4639m, and z=-6.6021m for the whole divertor (Fig.15); x=7.4024m, y=-0.4578 m, and z=-6.6206m for the cooling subsystem (Fig.17).

Finally, Table 4 summarizes the peak values attained by each component of the resultant Lorentz's forces and the resultant moments.

The results obtained here are coherent with the literature. For the same VDE, the resultant forces and moments on the whole divertor (Figs. 14 and 15) are qualitatively similar to those obtained in [5] and [7], where a simplified version of the divertor is used (note that in [7] the components are denoted in a different way). The agreement is excellent also quantitatively, with reference to the time interval before the injection of the Halo currents (t = 1.66 s). After that instant, the forces and moments evaluated here decay more slowly than those predicted in [7], probably due to the different time constants associated to the two models.

The results are also in agreement with [8], where the main component of the Lorentz's Force results to be the vertical one, as in this case. However, as pointed out in [8], the models are different and the force peaks appearing in [8] are higher than here (Fz raises up to 4 MN, Fx to 3 MN and Fy is negligible compared to these components).

Even the analytical estimations in [9] confirm that the most critical EM load is associated to the downward net vertical forces. In addition, for VDE such loads are not so influenced by the aspect ratio of DEMO tokamak, as it happens for other events.

The results provided in Figs.16 and 17 report the loads expected on the whole cooling system (the peaks are summarized again in Table 4). Note that on this system the vertical and radial components of the resultant forces are comparable, whereas the main component of the moments remains the vertical one. This behaviour are to be taken into account for properly design the supports of the cooling system to cassettes and VV.

To this end, a sensitivity analysis is carried out aimed at verifying the impact on the EM loads of the electrical resistivity values of the materials used for the supports inserted between the vertical targets and the cassettes, between the cooling system and the VV, and between the cassettes to the VV. The considered configurations are listed in Table 5 (Case 1 is the configuration so far discussed, hereafter assumed as the reference condition).

 https://doi.org/10.1016/j.fusengdes.2021.112999

The status of conductivity of these supports has an obvious impact on the paths of the currents flowing inside the divertor as well as those flowing from and to the VV.

The resistivity values for the materials listed in Table 5 can be found in Table 1, except for copper, for which a resistivity of $1.68 \cdot 10^{-8}$ Ωm is here assumed. The results of the sensitivity analysis are summarized in Tables 6 and 7, where the peaks of forces and moments are reported for the whole divertor and for the cooling system only, respectively.

Compared to the reference case (Case 1), the configurations of Cases 2-4 do not significantly change the peaks of the main components of forces and moments for the whole divertor assembly (the vertical ones), as shown in Table 6. A slight reduction of loads is observed for Case 4 for the radial and poloidal components of the forces.

Table 5. Electrical configurations of the supports for the analyzed cases (case 1 is the reference condition).

	Vertical target to cassette	**Cooling system to VV**	**Cassettes to VV**
Case 1	Conducting (AISI 316 SS)	conducting (AISI 316 SS)	Conducting (Ti-6Al-4V)
Case 2	Conducting (AISI 316 SS)	conducting (AISI 316 SS)	Conducting (Cu)
Case 3	Conducting (AISI 316 SS)	Insulating	Conducting (Ti-6Al-4V)
Case 4	Insulating	conducting (AISI 316 SS)	Conducting (Ti-6Al-4V)

Table 6. Peak values of the resultants of Lorentz's forces and moments on the divertor assembly in the analyzed case studied, defined in Table 5 (VDE_DOWN_74ms event).

	Fx [kN]	**Fy [kN]**	**Fz [kN]**	**Mx [kNm]**	**My [kNm]**	**Mz [kNm]**
Case 1	**-442.5**	**-451.3**	**-1283**	**-2104**	**-542.8**	**-3183**
Case 2	-449.8	-450.2	-1342	-1929	-478.7	-3185
Case 3	-360.4	-408.5	1209	-2125	-447.3	-3159
Case 4	-367.4	-393.9	1201	-2129	-439.2	-3053

Table 7. Peak values of the resultants of Lorentz's forces and moments on the cooling system in the analyzed case studied, defined in Table 5 (VDE_DOWN_74ms event).

	Fx [kN]	**Fy [kN]**	**Fz [kN]**	**Mx [kNm]**	**My [kNm]**	**Mz [kNm]**
Case 1	**-127.45**	**34.17**	**125.36**	**-112.98**	**-154.71**	**-314.56**
Case 2	-122.81	33.85	121.28	-114.09	151.89	-310.27
Case 3	37.85	-6.41	-41.25	-59.88	-34.74	-304.39
Case 4	-4.56	1.66	5.57	3.94	4.37	-85.06

The different combinations of the conductivity values of the support may instead greatly reduce the EM loads associated to the cooling system (Table 7). Changing the conductivity of the support of cassette to VV (Case 2) does not have significant effect, but using insulating supports between the cassettes and the VV (Case 3) may reduce the peak of the higher component (F_z) of about 66%, while leaving almost constant the peak of the higher component of the moments (M_z). The best option to reduce both forces and moments on such subsystem is Case 4, namely choosing insulating supports between the cassettes and the vertical targets. In this case, the peak of all the components of forces and moments are reduced by more than one order of magnitude, with a reduction of about 95% on F_x and F_z and of about 74% on M_z.

A final study is devoted to the potential effect of the electrical conductivity of the water, that is supposed to be non conductive but can exhibit a low but non-zero conductivity in real cases. To this purpose, the value of 0.2 μS/cm is here assumed, taken from the properties of ITER IBED water [22]. However, the results in terms of forces and moments do not significantly change when assuming this value, compared to modelling the water as a perfect insulator. Indeed, the above conductivity is more than ten orders of magnitude lower than that of the pipe materials (see Table 1).

4. CONCLUSIONS

The EM loads acting on a divertor of the EU-DEMO machine and its cooling subsystem are here evaluated, with reference to a downward Vertical Displacement Event. The transient analysis is carried out on a 22.5° sector of EU-DEMO tokamak, by exploiting symmetry and periodicity of the solution. The model adopted here include a detailed description of the three divertors falling into the above sector (including supporting structures) and a coarser description of the main external components, such a vacuum vessel and blankets. The sources of eddy and Halo currents are given in terms of equivalent currents and fluxes associated to suitable layers and surfaces. These sources are derived by plasma simulations carried out with the CarMa0NL code.

The results in term of forces and moments acting on the whole divertor assembly highlight the main role of the vertical (downward) components, whose peaks are estimated as high as about 1290 kN and 3190 kNm, respectively. The radial and poloidal components of forces exhibit peak levels that are about 35% of the vertical component, whereas the same components of moments show peaks between 66% and 18% of the vertical component. The forces and moments acting on the cooling system may be relevant, attaining peaks

values of about 130 kN and 315 kNm. In this case, the radial forces are comparable to the vertical ones.

A sensitivity analysis is carried out to check the influence on the above loads of the conducting properties of the supports of the cooling pipes. It is shown that the forces and moments may dramatically be reduced to 30% of the original values, if the supports between the cooling system and the vacuum vessel are insulating, and to 4% of the original values, if the supports between the vertical targets and the cassettes are insulating.

Perspective work will address the impact of a more refined modelling of the material properties (for instance to include anisotropy and inhomogeneity when needed) and the impact of Maxwell force due to the presence of ferromagnetic materials.

ACKNOWLEDGMENTS

This work has been carried out within the framework of the EUROfusion Consortium and has received funding from the Euratom research and training programme 2014-2018 and 2019-2020 under grant agreement No 633053. The views and opinions expressed herein do not necessarily reflect those of the European Commission.

This work has been also supported in part by Italian MUR under PRIN grant 20177BZMAH".

REFERENCES

[1] G. Federici et al., Overview of the design approach and prioritization of R&D activities towards an EU DEMO, Fusion Engineering and Design, 109-111 (2016) 1464-1474.

[2] G. Federici et al., Overview of the DEMO staged design approach in Europe, Nuclear Fusion 2019 in press https://doi.org/10.1088/1741-4326/ab1178.

[3] F. Villone et al., Report on 3D Electromagnetic analysis of DEMO disruptions, EFDA_D_2MUNQ3.

[4] G. Mazzone et al., Eurofusion-DEMO - Cassette Design and Integration, Fusion Engineering and Design, 157 (2020) 111656.

[5] J.H.You, et al., "Progress in the initial design activities for the European DEMO divertor: Subproject "Cassette", Fusion Engineering and Design, 124 (2017) 364-370.

[6] M. Roccella, DEMO baseline 2017 EM analysis: Global DEMO EM analysis – EM DGM_2019_confAandConfB", EFDA_D_2N9KV5.

[7] M. Roccella, DEMO baseline 2018 EM analysis: "EM DGM including TFCs and EM analyses of Plasma disruptions plus TFCs FD, EFDA_D_2MBYNY.

[8] V. Cocilovo, G. Ramogida, Simulation of electromagnetic VDE plasma effects on divertor structures of DEMO, Fusion Engineering and Design, 136 (2018) 1452-1460.

[9] C. Bachmann, Estimate of the Main EM Loads in DEMO Depending on the Aspect Ratio, EFDA_D_2MBSE3.

[10] S. El Shawish, L. Giannone, A. Kallenbach, Study of electromagnetic disruption forces for plasma detachment measurements in DEMO, Fusion Engineering and Design, 138 (2019), 372-378.

[11] S. Kwon, K. Im, Y. Lee, S.-H. Hong, Preliminary electromagnetic loads calculation for the divertor of K-DEMO, Fusion Engineering and Design, 146, Part B (2019) 2135-2139.

[12] U. Bonavolontà et al., EU-DEMO divertor: Cassette design and PFCs integration at pre-conceptual stage-Fusion Engineering and Design, 159 (2020) 111784.

[13] ITER Materials Properties Handbook, ITER document no. D_2NRCSB

[14] ITER Materials Properties Handbook, Material CuCrZr, Property: Electrical Resistivity, ITER document no. G 74 MA 16.

[15] Material Property Handbook on EUROFER97, 2MT9X8_v1_0.

[16] K. Mergia, N. Boukos, "Structural, thermal, electrical and magnetic properties of Eurofer 97 steel", Journal of Nuclear Materials, 373 (2008) 1-8.

[17] I. A. Maione, M. Marracci, B. Tellini, Study on remanent magnetization of Fe-9Cr steel and its effect on in-vessel remote handling for future fusion reactors, Fusion Engineering and Design, 88 (2013) 2092-2095.

[18] R.A. Kempf, et al., "Correlation between radiation damage and magnetic properties in reactor vessel steels," Journal of Nuclear Materials, 445 (2014) 55-62.

[19] T. Hender et al., "MHD stability, operational limits and disruptions" Nucl. Fusion 47 (2007) S128

[20] F. Villone, L. Barbato, S. Mastrostefano, and S, Ventre, Coupling of nonlinear axisymmetric plasma evolution with three-dimensional volumetric conductors, Plasma Phys. Control. Fusion, 55 (2013) 095008.

[21] www.ansys.com

[22] ITER System requirement Document, SRD-26_PH, IDM 2823A2, 2013.